METHODOLOGY FOR INCREASED PRECISION IN SATURATION TRANSFER ELECTRON PARAMAGNETIC RESONANCE STUDIES OF ROTATIONAL DYNAMICS

THOMAS C. SQUIER AND DAVID D. THOMAS
Department of Biochemistry, University of Minnesota Medical School, Minneapolis, Minnesota 55455

ABSTRACT Microsecond rotational motions of nitroxide spin labels are measured primarily with saturation transfer electron paramagnetic resonance (ST-EPR). In the present study we have used model system experiments to quantitatively evaluate different ST-EPR spectral parameters, both in-phase and out-of-phase, with an emphasis on techniques for suppressing the interference from weakly immobilized probes. Analyses of both systematic and random errors show that maximum sensitivity to small changes in correlation time and minimum ambiguity of interpretation are best achieved by combining measurements of both spectral line-shape, i.e., the ratio of line-heights, and spectral intensity, i.e., the absolute amplitude of either a position within a spectrum or a spectral integral. Errors in the measurement of correlation times for the two types of parameters tend to be complementary. Integrated intensity parameters are particularly useful in measuring microsecond probe motions in the presence of weakly immobilized components. We confirm that integrated intensity parameters are sometimes effective in rejecting signals from weakly immobilized probes, but the effectiveness of this rejection is more limited than previously supposed and depends on the type of parameter being measured. We describe procedures for evaluating and minimizing errors due to weakly immobilized probes, emphasizing the advantages of a new kind of intensity parameter obtained from integrated in-phase spectra. We provide detailed descriptions of experimental procedures, along with calibration plots of the most useful spectral parameters vs. rotational correlation time, which should make it possible for workers in other laboratories, using different instruments and sample geometries, to reproduce spectra quantitatively and to make accurate correlation time measurements.

INTRODUCTION

Saturation transfer electron paramagnetic resonance (ST-EPR) is a powerful tool for studying the rotational dynamics of nitroxide spin labels in the biologically important microsecond-to-millisecond time domain. In general, a saturation transfer EPR experiment is one designed to detect the decreased saturation caused by microsecond rotational motions. The development of ST-EPR methods is thus primarily the development of spectral detection and display methods that are optimally sensitive to saturation, preferably in a way that maximizes motional effects and minimizes others.

The first attempts to exploit these principles involved the performance of EPR experiments by conventional methods (V_1, using the terminology of Thomas et al., 1976), except that the microwave power was turned up to achieve a high enough H_1 value for partial saturation of the spin system (Hyde et al., 1970; Seidel, 1973; Goldman et al., 1973). This type of experiment is sometimes referred to as steady-state or continuous-wave (CW) saturation. Changes in τ_r that were not detectable at low (nonsaturating) power, presumably because they were in the microsecond time range, were detectable under saturating conditions. Although it was noted that absolute spectral intensities are sensitive to the increased saturation accompanying very slow motions (Seidel, 1973), attention was focused on line-shape changes, which were found to be relatively small (Hyde et al., 1970; Seidel, 1973; Goldman et al., 1973).

Subsequently, Hyde and Dalton (1972) reported dramatically improved line-shape sensitivity to microsecond rotation when the reference phase on the phase-sensitive detector was turned out-of-phase (phase-quadrature) relative to the modulation field, i.e., 90° away from the in-phase setting that maximizes the signal in the conventional EPR experiment. Their detection scheme was modified by Hyde and Thomas (1973) and refined by Thomas et al. (1976) to produce the methodology that has been standard for ST-EPR during the past decade. The detection scheme is designated V_2' (absorption, second harmonic, out-of-phase), and a quantitative analysis of V_2' spectra has involved the measurement of line-shape (line-height ratio) parameters, which take advantage of the variation of motional sensitivity as a function of spectral position (Thomas et al., 1976). However, as in the case of previous V_1 saturation studies, these line-shape parameters are not sensitive to the changes in overall spectral intensity that saturation transfer causes.

A number of possible improvements in this methodology

have been suggested in recent years, including the introduction of alternative methods of data interpretation and spectral parameterization (reviewed by Hemminga, 1983; Dalton, 1985; Thomas, 1985, 1986). In particular, methods have been proposed to overcome the interference that often occurs due to the presence of small amounts of weakly immobilized probes (i.e., probes having nanosecond rotational correlation times and low order parameters), which can distort line-shapes. Although spectral subtraction procedures can be used to remove the spectral contribution from weakly immobilized probes (Fajer, 1983; reviewed in Dalton, 1985), in practice it is difficult to model accurately the weakly immobilized spectral component. Therefore, it has been proposed (Evans 1981; Horvath and Marsh 1983) that the integrated intensity of V'_2 can suppress signals from weakly immobilized probes, resulting in less ambiguous measurements.

In the present study, we use model systems to study the effects of isotropic rotational motion, exploring a wider range of spectral displays and parameters than has previously been studied quantitatively. In order to study the effects of weakly immobilized probes (and learn how to suppress them), we have recorded spectra not only from spin-labeled hemoglobin, probing the usual microsecond time range, but also from TANOL, probing the sub-microsecond time range. We consider spectral parameters depending on both line-shape and intensity, from both in-phase and out-of-phase spectra. In addition to the integrated intensity of V'_2, we also report analysis of the double-integrated intensity of the saturated V_1 spectrum, and the absolute intensity of single positions in the V_2 and V'_2 spectra. Motionally sensitive spectral parameters are evaluated, and recommendations are made concerning the relative merits of their use, based on a quantitative analysis of the errors in determining correlation times with different parameters under typical conditions. We emphasize methodology that can be conveniently and precisely applied, using commercially available instrumentation, and that should produce comparable results from instruments in different laboratories, using different sample geometries. Thus the plots of spectral parameter values vs. rotational correlation time presented in this study can serve as generally applicable calibration plots.

METHODS

Chemicals

All spin labels (see Fig. 1) were from Aldrich (Milwaukee, WI). Sec-butyl benzene was from Aldrich. All spin labels were made into 0.10 M stock solutions in dimethylformamide (DMF) and stored at −70°C for up to six months. Spectral grade glycerol (≥99.9%) was purchased from Fisher Scientific Co. (Pittsburgh, PA). DMF (from Fisher Scientific Co.) was stored with molecular sieves to prevent water contamination.

Preparation of Model-System Samples

Reference EPR spectra were obtained from model systems undergoing isotropic rotational diffusion with known rotational correlation times.
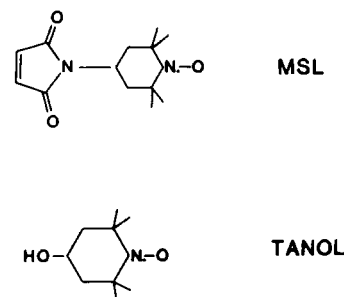

FIGURE 1 Spin labels used in this study. MSL (4-Maleimido-2,2,6,6-tetramethyl piperidinooxyl) was bound covalently to hemoglobin in order to obtain a model compound for the study of microsecond rotational motion, while TANOL (4-Hydroxy-2,2,6,6-tetramethyl piperidinooxyl) in aqueous glycerol and sec-butyl benzene solvents, and was used to obtain a calibration for weakly immobilized probes.

Hemoglobin, labeled with the maleimide spin label 4-maleimido-2,2,6,6-tetramethyl-4-piperidinooxyl, designated MSL-Hb, was dissolved in aqueous glycerol solutions for studies of the microsecond time range, and TANOL (4-hydroxy-2,2,6,6-tetramethyl piperidinooxyl) was dissolved in either aqueous glycerol solutions or sec-butyl benzene (SBB) for studies of the sub-microsecond time range.

Human oxyhemoglobin was prepared essentially as reported by Thomas et al. (1976). Red blood cells were washed in 0.9% NaCl and lysed in distilled water (0–4°C). The resultant red cell ghosts were pelleted, leaving a supernatant containing purified hemoglobin. The hemoglobin concentration was determined from its visible absorption spectrum (Benesch et al., 1965). All hemoglobin solutions discussed below contained 0.10 M sodium phosphate (adjusted to pH 7.0 at 4°C).

Hemoglobin was labeled specifically (Ohnishi et al., 1966) at both β-93 sulfhydryls with MSL at a ratio of 2.5:1 (MSL/Hb) overnight (18 h) at 0°C (Thomas et al., 1976; Ohnishi et al., 1966). The reaction was 80% complete (1.6 moles of spin label bound per mole of hemoglobin) as judged by the intensity of the remaining EPR signal component due to free (unreacted) probes. The EPR spectrum after dialysis (to remove unreacted label) resembles a "powder" spectrum, with a single spectral component corresponding to "strongly immobilized" spin labels, indicating a rotational correlation time $\tau_r > 10^{-8}$ s. The spin-labeled hemoglobin was concentrated, using a PM-10 Amicon filter (Amicon Corp., Scientific Systems Div., Danvers, MA) under nitrogen, to a concentration of 3 mM. EPR samples were prepared by diluting this concentrated solution into glycerol/buffer solutions (measured wt/wt) to a final hemoglobin concentration of 0.3 mM, except for the sample containing 95% glycerol (vol/vol), which contained 0.15 mM hemoglobin. These solutions are stable at −20°C for years. The solvent viscosities were measured and found to be in good agreement with tabulated values (Weast, 1961; Ibert, 1970).

In order to obtain reference spectra corresponding to no detectable rotational motion (the rigid limit), spectra were obtained from MSL-Hb that was either lyophilized or precipitated in ammonium sulfate (Thomas et al., 1976). Some samples of the latter were cross-linked with 10 mM glutaraldehyde overnight, in order to determine whether there was any residual segmental flexibility in this "rigid-limit" sample. The above spectra were all similar, providing a reliable estimate of the rigid-limit. Each point at infinite τ_r in the parameter plots (Fig. 3) is the mean value for these three rigid-limit samples. The intensity parameters were identical within experimental error for all three samples. Although the lineshapes were nearly identical, there were small differences in the center of the spectrum, suggesting that the rigid limit remains the major uncertainty in the ST-EPR experiment. There was no change in the spectrum of ammonium sulfate precipitated hemoglobin on cross-linking, suggesting that these small spectral differences are not motional effects, but are due to differences in the dielectric properties of the samples.

The solvent viscosities for SBB were obtained from tables (Barlow et

al., 1966). The concentration of TANOL was kept at or below 10^{-4} M in aqueous glycerol solutions and 10^{-5} M in SBB. These concentrations were dilute enough to prevent Heisenberg exchange, since further dilution had no effect on the line-shapes or saturation properties of the spectra.

Deoxygenation of Samples

Reference spectra were recorded in the presence or absence of molecular oxygen. Every encounter within 4.5 Å between a spin label and O_2 leads to a Heisenberg exchange event, which removes spectral saturation (Hyde and Subczynski, 1984). Oxygen was removed from experimental samples using either gas-permeable sample cells purged with N_2 (Popp and Hyde, 1981), or oxygen-scavenging enzymes. The latter method involved the use of either glucose, glucose oxidase, and catalase (Eads et al., 1984); or catechol and 3,4-protocatechuate dioxygenase (used with hemoglobin to avoid formation of met-hemoglobin from the H_2O_2 generated by glucose oxidase). EPR spectra (V_1, V_2', etc.) of MSL-Hb samples in solutions having a viscosity ≥ 0.2 poise were insensitive to the removal of molecular oxygen, implying that (a) the collision rate of O_2 with the spin label is sufficiently slow to eliminate Heisenberg exchange due to interactions of the spin-labels with molecular O_2 and (b) the rotational motion is not affected by the small conformational difference between oxy- and deoxy-hemoglobin.

Instrumentation

EPR experiments were performed on a Varian E109 X-band spectrometer (Varian Associates, Inc., Palo Alto, CA). All experiments were done in the absorption mode (V_1) using a TE_{102} cavity (Varian E231). The Zeeman field was modulated either at 50 kHz (V_2 or V_2'), with a peak-to-peak modulation amplitude of 5.0 Gauss, or at 100kHz (V_1 or V_1'), with a modulation amplitude of 2.0 Gauss. The signal was detected using a phase-sensitive detector either in-phase (V_1 or V_2) or 90° out-of-phase (V_1' or V_2') (see Thomas et al., 1976; reviewed by Dalton, 1985; Thomas, 1985, 1986). Spectral scans were digitized with 516 points per 100-Gauss scan (Lipscomb and Salo, 1983).

H_1 Calibration

The extent of saturation, which determines the intensity and shape of the V_2' spectrum, depends primarily on the intensity of microwave radiation (H_1, where the microwave radiation field is $2H_1 \cos \omega t$) that depletes the ground state, and only secondarily on saturation transfer that reduces the effects of this radiation by transferring saturation to other (not irradiated) spectral positions. Saturation reduces the steady-state magnetization, M_z, below the Boltzmann equilibrium distribution value, M_o, according to:

$$M_z/M_o \equiv 1/(1 + S),\qquad(1)$$

where $S = \gamma^2 H_1^2 T_1 T_2$ for a homogeneously broadened line in the absence of saturation transfer, where H_1 is the microwave field amplitude at the sample, T_1 is the spin-lattice relaxation time, and T_2 is the spin–spin relaxation time. Thus, in order to ensure that changes in saturation depend only on saturation transfer, it is desirable to keep H_1, T_1, and T_2 constant for spectra that are to be compared. It is often assumed that T_1 and T_2 are nearly constant. Time-resolved EPR measurements indicate that this assumption is generally justified in the absence of oxygen or submicrosecond motions (Hyde and Dalton, 1979; P. Fajer and D. Thomas, unpublished), although the most rigorous approach would require the measurement of these relaxation times for each sample. H_1 is therefore the most important variable to control in an ST-EPR experiment. The standard value of H_1 used by most workers is 0.25 Gauss, which can correspond to a power setting anywhere from 1 to 100 mW, depending on the resonator and sample characteristics. The accurate setting of microwave power so that $H_1 = 0.25$ Gauss (or any other desired value of H_1) requires three steps (All experiments and calibrations are performed with the reference arm on and the cavity critically coupled.).

Saturation of standard. The most reliable means of measuring H_1 is to measure S for a standard sample, for which T_1 and T_2 are precisely known (Thomas et al., 1976; Fajer and Marsh, 1982). The sample of choice is a deoxygenated solution of peroxylamine disulfonate ("PADS" or "Fremy's salt"), 0.9 mM in 50 mM K_2CO_3 at 20°C. In this sample, T_1 and T_2 are equal and are easily determined from the linewidth of the V_1 spectrum in the absence of saturation (Kooser et al., 1969), resulting in a straightforward calculation (p. 590 in Poole, 1983) of H_1 (1/2), the value of H_1 at which the V_1 spectral line-height (peak-to-peak) is half of its unsaturated value.

$$H_1(1/2) = S(1/2)/(\gamma T_2) = [2^{(2/3)} - 1]^{1/2}/(\gamma T_2)$$
$$= 0.664\ \Delta H_{pp},\qquad(2)$$

where ΔH_{pp} is the peak-to-peak linewidth (in Gauss) of the V_1 spectrum in the absence of saturation, and γ is 1.76×10^7 rad/Gauss. For the standard PADS sample, a typical value of ΔH_{pp} is 0.161 Gauss, corresponding to $H_1(1/2) = 0.1069$ Gauss. If the power setting needed to obtain half saturation of the standard is designated $P_s(1/2)$, this permits the calculation of the constant

$$K = [H_1(1/2)]^2/[P_s(1/2)] = H_1^2/P_s\qquad(3)$$

for all values of H_1. As described below (in the discussion of Eqs. 4–6), the quality factor for the standard, Q_s, is also measured at this time. This determination of K and Q_s for the standard is performed once for each type of sample cell.

Calibration of P. The microwave power attenuator must be accurately calibrated, so that H_1 really is proportional to the square root of the nominal power setting. In most cases, this can be achieved by adjusting the attenuator display so that the cavity-tuning mode pattern shows no dip at the resonance frequency when the attenuator display indicates minimum signal (maximum attenuation). That H_1 is proportional to $P^{1/2}$ is verified by recording a signal (proportional to H_1) as a function of P from a nonsaturated sample (e.g., DPPH placed in the cavity stack). That the absolute power has not changed since the PADS calibration (i.e., that the klystron output has not changed and the attenuator control has not become uncalibrated) is verified by measuring the amplitude of the klystron mode pattern on the oscilloscope for a standard power setting. Alternatively, a microwave power meter can be used. The calibration of P is carried out before the PADS calibration, and occasionally thereafter (about once per month in our laboratory).

Q correction. A further correction must be applied every time a sample is inserted into the cavity, since the quality factor Q of the microwave cavity changes due to slight changes in the sample's shape, position, or dielectric constant. Unless the sample is very small (≤ 5 mm in length), the value of H_1 is heterogeneous over the sample, with the H_1 gradient primarily in a direction parallel to the standard line samples, so H_1 is an average value (Fajer and Marsh, 1982). We assume that any variation in the mean H_1 from one sample to another obeys the relationship

$$\langle H_1 \rangle^2 = C \cdot Q \cdot P,\qquad(4)$$

where $\langle H_1 \rangle$ is the mean microwave intensity integrated over the sample, P is the klystron power incident upon the sample, Q is the quality factor, and C is related to geometrical factors of the waveguide and cavity. We assume (as justified by experiments in Results) that the geometrical term C is constant for each type of sample cell, so that Q is the only variable to be determined for each individual sample. Q can be measured from $\Delta\nu$, the frequency separation of the klystron output, after critical coupling, at half height:

$$Q = \nu_o/\Delta\nu,\qquad(5)$$

where ν_o is the cavity resonance frequency. Then the power setting P required to obtain a desired $\langle H_1 \rangle$ is given by solving Eqs. 3–5 for P:

$$P = P_s \times (Q_s/Q) = K\langle H_1 \rangle^2 (\Delta\nu/\Delta\nu_s), \qquad (6)$$

where Q_s and K were determined previously for the standard.

Modulation Phase Setting

In V_2' experiments, the reference phase on the 100 kHz phase-sensitive detector is set 90° away from the conventional in-phase setting. The signal detected under these conditions (lagging in phase because of saturation) is typically much less intense than the in-phase signal that is to be rejected, so a much more precise setting is necessary than in conventional EPR. For example, if the in-phase signal (V_2) is 10 times as intense as the out-of-phase signal (a typical value), and no more than 5% error in the V_2' signal intensity can be tolerated (a typical requirement), the phase must be set with an accuracy of 0.5 degrees. This is possible if the following procedure is followed (reviewed in Thomas, 1985, 1986): The most intense (central) feature of the second harmonic signal is recorded at low power, typically corresponding to an H_1 value of 0.032 Gauss or less, to avoid saturation (and the accompanying phase lag). The phase is varied until an approximate null is achieved. The power is then turned up to correspond to $H_1 = 0.25$ G, and the gain is adjusted to give the desired V_2' signal height. For the final (fine) phase setting, the power is reduced again to a low (nonsaturating) level and the signal intensity (peak-to-trough) is recorded at two phase settings, approximately two degrees on either side of the approximate null phase value determined above. The precise value is determined and set by linear interpolation between these two settings to determine the phase corresponding to a null signal. The power is then turned up to the desired level ($H_1 = 0.25$ Gauss) and the V_2' spectrum is recorded. It is best to perform the final phase adjustment just before each V_2' measurement, with all spectrometer settings (especially gain), except power, set at the same values to be used in the V_2' experiment, since changes in gain and other settings can cause phase shifts (Thomas et al., 1976). In order to avoid phase drift during the recording of the spectrum (which can require acquisition times ranging from a few minutes to a few hours), it is advisable to warm up the instrument for several hours before starting experiments and to keep the ambient temperature constant (± 1°C) during the experiment.

Spectral Analysis

Measurement of T_2. The spin–spin relaxation time T_2 is related to the peak-to-peak linewidth ΔH_{pp} of the homogeneous Lorentzian distribution of spins (spin packet) at a single orientation (single resonance condition) under nonsaturating conditions (Carrington and McLachlan, 1967):

$$T_2 = 2/(3^{1/2} \times \gamma \times \Delta H_{pp}). \qquad (7)$$

Anisotropic proton super-hyperfine interactions lead to an apparent or effective line-width ΔH_{pp}^* considerably greater than the homogeneous line-width ΔH_{pp}, making a quantitative measurement of T_2 impossible. In the subnanosecond time range, the anisotropy is averaged and the proton super-hyperfine lines are resolved in the absence of O_2, so T_2 can be measured from Eq. 7.

Calculation of Correlation Times for Model Systems. It has been shown previously that the maleimide spin label is rigidly bound to hemoglobin, which behaves in aqueous glycerol solutions as a rigid sphere, undergoing isotropic Brownian rotational diffusion (Ohnishi et al., 1966; McCalley et al., 1972; Hyde and Thomas, 1973). Thus the spin label's (and hemoglobin's) rotational correlation time (in seconds) obeys the equation

$$\tau_r = \eta/T \times Z, \qquad (8)$$

where η is the viscosity in poise and T is the temperature in °K. The constant Z was determined to be 7.6×10^{-4} (Hyde and Thomas, 1973) for MSL-Hb by measuring τ_r from the conventional EPR spectrum in aqueous solution at 20°C (McCalley et al., 1972). Similarly, we assumed that TANOL obeys Eq. 8 in aqueous glycerol and sec-butyl benzene solutions, and Z was determined to be 2.9×10^{-7} from an analysis of the conventional EPR spectrum of TANOL in 70% (wt/wt) glycerol/water at 20°C, using the theory that relates line-height ratios to τ_r (Keith et al., 1970).

Measurement of Spectral Parameters

The dependence of EPR spectra on τ_r and other variables is quantitated by measuring various spectral parameters. In the present study, we discuss two general types of parameters, designated line-shape and intensity parameters. A line-shape parameter is the ratio of two line-heights within the same spectrum (always a V_2' spectrum in the present study). The line-height is measured at a spectral position with maximal sensitivity to motion, and this value is divided by the line-height at a less motion-sensitive position within the same V_2' spectrum. This has been the standard type of parameter used to analyze ST-EPR spectra, and the definitions used here are the same as described previously (Thomas et al., 1976). However, this normalization within the spectrum, in which both numerator and denominator depend on saturation and motion, prevents sensitivity to changes in the overall intensity of the spectrum that are caused by saturation transfer. An intensity parameter is obtained by dividing a saturated (motion-sensitive) line-height or spectral integral by a value from an unsaturated spectrum (insensitive to microsecond motion), and is thus sensitive to changes in overall intensity. As discussed below in Results, line-shape parameters show useful sensitivity to motion only for the V_2' display, whereas motion-sensitive intensity parameters can also be obtained from V_1 and V_2 spectra. The precise definitions of the parameters used will be given in Results.

RESULTS

Reference Spectra

Fig. 2 summarizes the sensitivity of ST-EPR to isotropic rotational diffusion, for four different spectral displays. This figure is a dictionary of reference spectra from the two model systems (with known correlation times) over the entire time range in which EPR is sensitive. This figure illustrates the effects of motion not only on line-shape (Thomas et al., 1976), but also on intensity, since the spectra within each column are normalized by dividing by $\iint V_1$ and H_1. Thus the difference (in both line-shape and intensity) between the solid (saturating power) and dashed (nonsaturating power) curves in each pair is due entirely to saturation effects. Line-heights used to define parameters are shown in Fig. 2 and defined below, but several important features are worth noting before proceeding to a quantitative parametric analysis. Note that the in-phase spectral intensities are decreased by saturation (hence increased by microsecond motion that causes saturation transfer), while the out-of-phase intensities are increased by saturation (hence decreased by microsecond motion). The conventional (V_1) EPR line-shape is maximally sensitive to rotational motion in the time range $10^{-11} < \tau_r < 10^{-7}$ s. Under saturating conditions (solid curves), the V_1 line-shape does show sensitivity to rotational motion in the microsecond time range (Goldman et

V_1 V_2 $\tau_r(\text{sec})$ V'_2 $\int V'_2$

L_{pp}

10^{-3}

10^{-5}

10^{-7}

10^{-9}

10^{-11}

x 0.10   x 0.10   x 0.10

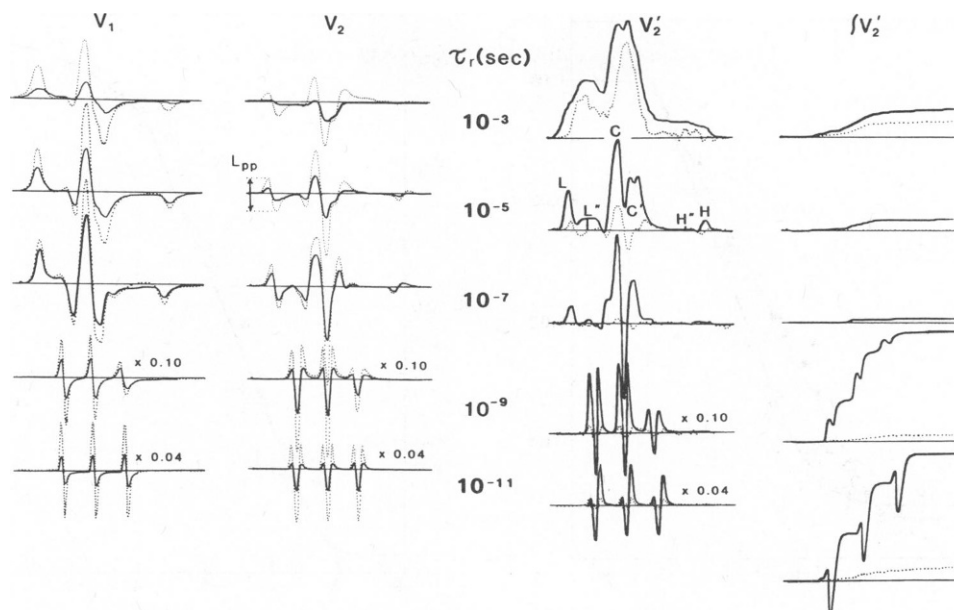x 0.04   x 0.04   x 0.04

L   L'   C   H'   H

FIGURE 2 Reference EPR spectra from model systems, demonstrating the effect of isotropic rotational motion on EPR spectral line-shapes and intensities. The spectra within each column are all normalized to the same spin concentration (divided by $\int\int V_1$) and divided by H_1, except where a different scale factor is indicated (i.e., the V_1, V_2, and V'_2 spectra at 10^{-9} and 10^{-11} s). From the top, the samples are Hb in 95% (vol/vol) glycerol, $-20°$C; 69% (vol/vol) glycerol, $-12°$C; 50% (vol/vol) glycerol, $30°$C, TANOL in 90% (wt/wt) glycerol, $30°$C; TANOL in H_2O, $20°$C. The spectral displays shown are V_1, V_2, V'_2, $\int V'_2$, and are explained in Methods. The out-of-phase spectra (i.e., V'_2) are taken at a factor of 20 larger gain. The spectra were all recorded at $H_1 = 0.25$ Gauss (solid line) and $H_1 = 0.032$ Gauss (dashed line), which correspond to saturating and nonsaturating power, respectively. The horizontal axis is the resonance field and the baseline represents a scan range of 100 Gauss for all spectra. The TANOL spectra are scaled down relative to the Hb spectra as indicated in the figure. Line-heights used to calculate parameters are defined as shown, with the following explanations: Unless the subscript $_{pp}$ is included, all line-heights are measured with respect to the baseline. L is a well defined (resolved) peak in V'_2 for 10^{-7} s $< \tau_r < 4 \times 10^{-4}$ s. For longer τ_r, when the L position is not clearly resolved, the L position at $\tau_r = 10^{-4}$ s is used. L'' is defined as the line-height at the field position 10 Gauss to the right of L. Similarly, H is the high-field line-height in V'_2, and H'' is 10 Gauss to the left. The C and C' features are the first peak and trough in the center of V_2. L_{pp} is the peak-to-peak height of the low-field line of V_2.

al., 1973), but this sensitivity is minimal, since the V_1 intensity is primarily at the turning points, where orientational resolution is minimal (Thomas et al., 1976; reviewed in Thomas, 1985, 1986; Dalton, 1985). The overall intensity of V_1 at saturating power (solid curves) clearly increases with motion, showing much more sensitivity to microsecond rotational motion than does the V_1 line-shape. The V_2 spectra are approximately derivatives of V_1 spectra and thus show similar τ_r dependence. V'_2 spectra have the unique property that both their line-shape and intensity are quite sensitive to motion, because the rigid-limit spectra have significant intensity at all spectral positions, not just near the turning points (Thomas et al., 1976). The decrease of the V'_2 intensity with microsecond motion is clear from inspection of the V'_2 spectra, but is even more striking in the display of the spectral integral ($\int V'_2$). Submicrosecond correlation times yield spectra that appear to have roughly equal intensity above and below the baseline, but Fig. 2 (lower right) shows that the integrated intensity can actually have a very large value. Therefore, this parameter can not always be assumed to be effective in suppressing signals from weakly immobilized probes, as previously proposed (Evans, 1981; Horvath and Marsh, 1983).

Spectral Parameter Plots from MSL-Hb (microsecond range)

Fig. 3 shows the τ_r-dependence of parameters from MSL-Hb spectra, based on the displays and line-heights defined in Fig. 2.

The V'_2 spectrum is analyzed using three types of parameters. (a) A line-shape parameter (L''/L, C'/C, and H''/H, plotted in Fig. 3 A, B, and C, respectively) is the ratio of two line-heights from V'_2. In each case, the numerator is the line-height that is most sensitive to motion within a spectral region, and the denominator is the least sensitive. (b) A line-height intensity from V'_2 is one of these motion-sensitive line-heights (the numerator from one of the three line-height ratios), normalized by dividing by a motion-independent parameter. The V'_2 line-height intensity plotted in Fig. 3 A is L'', normalized by dividing by $L_{pp} \cdot \Delta H_{pp}^2/H_1$ at low power, which is independent of motion in the microsecond range. Alternatively, $\int\int V_1$ (low power) could be used as a normalization parameter, yielding a curve with an identical shape. L'' is sensitive to a greater range of τ_r values than is L''/L, since both L'' and L increase with τ_r. (c) The integrated intensity parameter derived from V'_2 is the integral of the spectrum ($\int V'_2$),
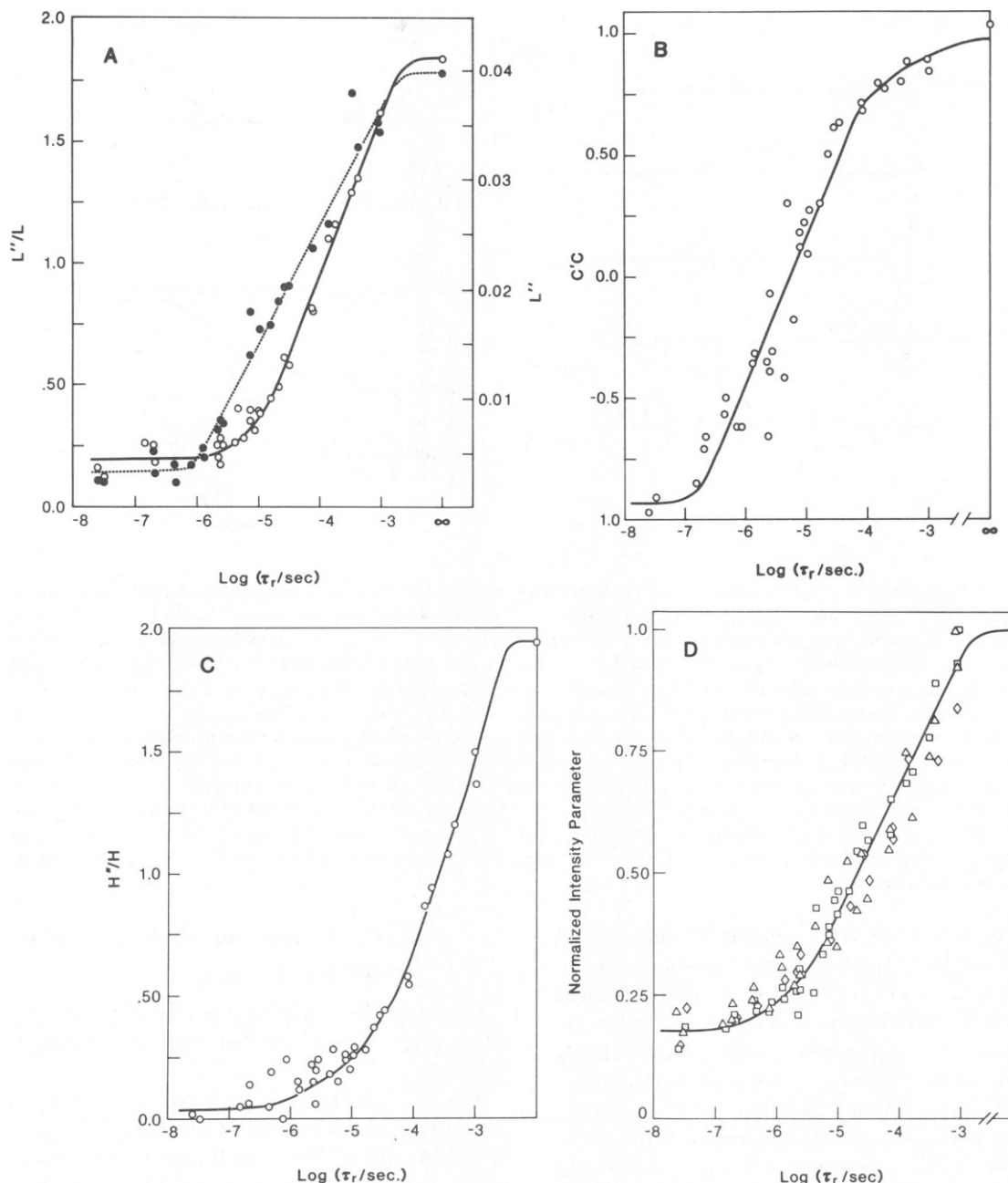
FIGURE 3 Dependence on microsecond τ_r values of parameters derived from ST-EPR spectra of MSL-Hb (Fig. 2, top). Correlation times τ_r were calculated with Eq. 8. Line-heights are defined in the legend of Fig. 2, and the parameters calculated from them are defined in the text. Open circles in A, B, and C are line-shape parameters from V_2'. L'', the spectrally resolved line-shape parameter from V_2', is plotted in A (solid circles, scale at *right*). D shows the intensity parameters $\int V_2'$, S_i', and S_r', all normalized relative to their rigid-limit values, which are 0.43, 1.2 and 1.2, respectively.

normalized as in Fig. 2 (right), by dividing by $\iint V_1/H_1$ at low power, a normalization parameter that is always independent of motion. Spectra were digitized with 516 points per 100 Gauss, and the V_1 field amplitudes were $H_m = 2$ Gauss and $H_1 = 0.032$ Gauss; any deviation from these standardized conditions would necessitate a proportional correction (or renormalization to the rigid-limit value) before the plot of this parameter in Fig. 3 D would

be directly applicable. None of the other parameters plotted in Fig. 3 have this kind of potential scale factor ambiguity.

Two other intensity parameters, both obtained from in-phase spectra, are plotted in Fig. 3 D. (Since in-phase spectra have line-shapes that are insensitive to motion, no line-shape parameters are plotted from in-phase spectra.) The integrated intensity parameter derived from V_1 is S_i',

which is defined as

$$S'_i = [\iint V_1(H_1 = 0.032 \text{ Gauss})/H_1]$$

$$/[\iint V_1(H_1 = 0.25 \text{ Gauss})/H_1] - 1. \quad (9)$$

The rationale for this definition is as follows: Neglecting passage effects, $\iint V_1$ should be proportional to M_z, so that S'_i is the apparent value of the saturation factor S (Eq. 1). That is, the extent to which S'_i is less than S is a direct measure of saturation transfer. When expressed in this form, this parameter has essentially the same motional dependence as $\int V'_2$, which is expected, since the latter is roughly porportional to saturation. Following a similar rationale, the line-height intensity parameter derived from V_2 is

$$S'_r = \langle [L_{pp}(H_1 = 0.032 \text{ Gauss})/(H_1)]$$

$$/[L_{pp}(H_1 = 0.25 \text{ Gauss})/H_1]\rangle^{2/3} - 1, \quad (10)$$

where the subscript indicates that this parameter is spectrally resolved, in contrast to the integrated saturation parameter S'_i. As expected, these two in-phase saturation parameters have a similar τ_r dependence (Fig. 3 D). An alternative (and essentially equivalent) parameter could be derived from any of the other line-heights in V_1 or V_2.

The parameters plotted in Fig. 3 all have similar sensitivity to microsecond rotational motion, although the expected differences are observed among the spectrally resolved line-shape parameters, due to the different orientational resolution in different spectral regions (Thomas et al., 1976). Thus the choice of the preferred parameter in a given case will depend on the likely sources of experimental errors and the parameters' relative sensitivity to these errors, as discussed in the remainder of this study.

Spectral Parameter Plots in the Submicrosecond Time Range

Fig. 4 shows the effects of submicrosecond rotational motion, obtained from the TANOL model system. Although motional averaging effects in conventional (unsaturated) EPR spectra are still the best indicator of nsec rotational motions, it is essential to quantitate the effects of these rapid motions on ST-EPR spectra, in order to assess
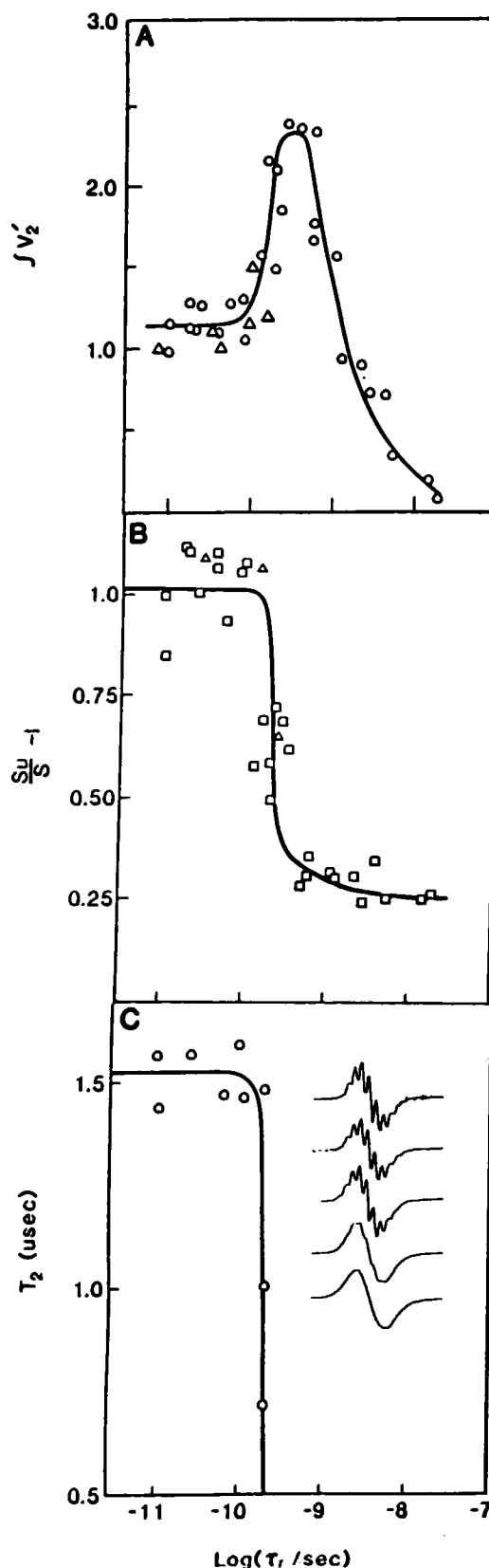

FIGURE 4 Dependence on submicrosecond τ_r values of parameters derived from spectra of TANOL (Fig. 2, bottom; and Fig. 4, inset). The solvent was either aqueous glycerol (O or □, varying glycerol concentration and T) or sec-butyl benzene (△, varying T). Correlation times τ_r were calculated with Eq. 8. A: SV'_2; B: S'_i; C: T_2. T_2 was calculated using the central proton hyperfine feature of the $m_I = 0$ line from the V_1 spectrum (see inset) using Eq. 7 for both TANOL in aqueous glycerol and SBB. For the spectra in the inset, the temperature was 20°C and the glycerol concentration was varied to obtain τ_r values, top to bottom, of 0.01, 0.03, 0.06, 0.33, and 0.60 ns.

the potential interference from weakly immobilized probes. The integrated V'_2 intensity ($\int V'_2$) is plotted vs. τ_r in Fig. 4 A. As τ_r decreases, this parameter increases dramatically, becoming a maximum at $\tau_r = 10^{-9}$ s. The integrated V_1 saturation parameter (S'_1) is analyzed in Fig. 4 B. Again, saturation increases with decreasing τ_r, but this increase occurs more abruptly at shorter τ_r, and no maximum is observed. These results, including the difference in τ_r-dependence between the two parameters, are not dependent on solvent properties, since the same results were obtained in SBB as in aqueous glycerol. In fact, essentially the same results were obtained for fatty acid spin labels in castor oil (data not shown).

In an effort to understand these saturation effects (Fig. 4 A, B), we measured T_2 for the same samples (Fig. 4 C). The inset in Fig. 4 C shows the center nuclear hyperfine feature from spectra of TANOL in aqueous glycerol under nonsaturating conditions at different τ_r. The proton super-hyperfine splittings are resolved for $\tau_r < 3 \times 10^{-9}$ s, permitting the measurement of T_2 from the linewidth (Eq. 7), and these values are plotted in Fig. 4 C. It is apparent that the increase of spectral saturation (as τ_r decreases) is coincident with an increase in T_2. There is a particularly good correlation between T_2 and the V_1 saturation parameter S'_1, consistent with the prediction that S'_1 should be proportional to T_2 (Eq. 1). The largest changes occur when τ_r approaches the Larmour frequency. The different dependence of $\int V'_2$ is not readily explained, but it is not surprising that the saturation properties of V'_2 are more complex than those of V_1.

Effects of Weakly Immobilized Probes on the Measurement of Microsecond Correlation Times

In order to determine quantitatively the error caused by the presence of a small fraction of weakly immobilized probes (i.e., probes where $\tau_r < 10^{-8}$ s) in the measurement of a microsecond correlation time by ST-EPR, we have analyzed composite spectra in which the major component is a spectrum of MSL-Hb (strongly immobilized) and the minor component is a spectrum of TANOL (weakly immobilized). Fig. 5 illustrates the production of one of these two-component spectra. The weakly immobilized component comprises only 5% of the total spins, and the V_1 spectrum does not differ markedly from that expected for strongly immobilized probes. However, when this composite spectrum is analyzed using the parameter plots in Fig. 3, the estimated τ_r values vary widely from each other and from the known τ_r of the MSL-Hb sample (see legend). We have performed this analysis on a wide range of composite spectra, and have found that the resulting errors in τ_r measurement depend on the actual τ_r values for both components, the mole fractions, and the parameter measured.

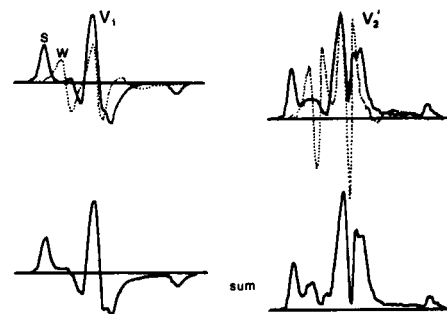These results are summarized in Table I. In this table,

FIGURE 5 Effect of weakly immobilized probes on ST-EPR (V'_2) spectra. *Top:* MSL-Hb in 90% glycerol (vol/vol) at 20°C (solid line; $\tau_r = 7.2\ \mu s$) and from TANOL in 90% glycerol (wt/wt) at 10°C (dashed line; $\tau_r = 4.7$ ns). The TANOL spectrum, which is meant to simulate a weakly immobilized component, has been normalized to the same spin concentration and then multiplied by a gain of 0.2 relative to that of MSL-Hb. *Bottom:* a composite of the top two spectra, containing 95 mol % of the Hb spectrum and 5 mol % of the TANOL spectrum. The τ_r values estimated from this composite spectrum (in μs) using different parameters are 37 (L''/L), 8.0 (C'/C), 17 (H''/H), 16 (L''), 8.0 ($\int V'_2$), 6.9 (S_i), 7.2 (S'_i).

TABLE I
EFFECTS OF WEAKLY IMMOBILIZED PROBES ON ST-EPR PARAMETERS
ST-EPR PARAMETER

τ_r(W)		L''/L	C'/C	H''/H	$\int V'_2$	S'_i	W/S = 1.0 % Spins
0.25 ns	a.	9.2	9.0	1.8	3.5	0.18	3.4%
	b.	75	−3.6	4.2	4.9	0.17	
	c.	5.4	−16	−0.2	2.2	−0.01	
0.96 ns	a.	16	4.7	1.6	3.8	0.04	5.0%
	b.	82	−4.1	4.5	2.8	−0.04	
	c.	3.6	−22	0.1	2.1	−0.10	
2.0 ns	a.	40	3.0	8.1	4.2	0.08	10%
	b.	86	−5.4	5.4	4.2	−0.12	
	c.	3.1	−28	3.3	1.8	−0.21	
4.7 ns	a.	70	4.1	9.3	2.8	0.06	32%
	b.	12	−6.8	5.2	1.8	−0.56	
	c.	4.6	−46	5.6	0.3	−1.11	
12.8 ns	a.	6.5	5.2	12	1.2	0.08	49%
	b.	−30	−19	11	0.8	−2.6	
	c.	3.5	−210	5.5	−4.3	−17	
Average		30	26	5	3	2	

The tabulated values for the different ST-EPR parameters, except S'_i, which was insensitive to W, are $= \delta[\tau_r/\tau_{ro}]/\delta(W/S)$, where τ_r and τ_{ro} are the correlation time values measured before and after the addition of a weakly immobilized spectral component (obtained from TANOL) to a MSL-Hb spectrum, as illustrated in Fig. 5. The parameters in columns 2–6 are defined in Figs. 2 and 3. The actual error in τ_r can be determined by multiplying the tabulated value by the actual value of W/S (up to a W/S value of ~2). The weakly immobilized component is characterized by τ_r(W) (column 1) and by W/S (defined in Fig. 2). The errors due to each of the weakly immobilized components are shown above for each of three different MSL-Hb samples, having τ_{ro} values of 0.2 $\mu s(a)$, 7.2 $\mu s(b)$, and 140 $\mu s(c)$. The values in the bottom row are the averages of all values in each column. The errors tabulated would occur from a line-height ratio (W/S) of 1.0 in the composite spectrum; the final column gives the mole fraction of the W component required to produce this change.

for each combination of component spectra (in which τ_{ro} is the actual correlation time of the hemoglobin sample and $\tau_r(W)$ is the correlation time of the weakly immobilized (TANOL) component, errors are expressed in terms of the fractional deviation of the estimated τ_r value from τ_{ro}, given a W component whose line-height is equal to that of the strongly immobilized component (W/S = 1 in Fig. 5, left). We have given the errors due to a constant line-height rather than a constant mole fraction, since it is W/S that is most directly measured from the spectrum. The corresponding mole fractions are given in the last column of Table I. Errors are generally large for the most commonly measured V'_2 line-height ratios L''/L and C'/C, but are much less for the line-height ratio H''/H, and even less for the integrated intensity parameters. Of the two intensity parameters, S'_i (from V_1) is clearly superior to $\int V'_2$ in its insensitivity to W.

Variation of Sample Geometry

The reference spectra in the present paper are useful for researchers in other laboratories only if similar results are obtained with different sample cells. Fig. 6 shows spectra of MSL-Hb in the three most commonly used line sample cells, which all have significantly different shapes and volumes. When the procedures described in Methods are used to ensure that $\langle H_1^2 \rangle$ is constant, especially the correction for differences in Q, identical spectra are obtained from the three cells (Fig. 6 A and Table II). However, when the microwave power P, not H_1, is kept constant, large variations are observed in both line-shape and intensity (Fig. 6 B). Thus the parameter plots in Fig. 3 can be used reliably for any line sample, provided that the recommended procedures are followed for keeping $\langle H_1^2 \rangle^{1/2} = 0.25$ Gauss. Preliminary studies indicate that similar V'_2 spectra are obtained with the Bruker ER200D spectrometer as well, although there may be some additional systematic errors in the Bruker instrument (due to modulation phase shifts) that prevent spectra from being identical to those obtained on the Varian E109 spectrometer used in the present work (M. Johnson, personal communication).

The lens effect, i.e., the focusing effect that water has on microwaves, can result in an increase in the H_1 value in an aqueous sample (Sarna and Lukiewicz, 1971). In principle, these effects might cause H_1 variation due to variation in sample volume, shape, and dielectric constant, despite the Q-correction described in Methods. However, our results indicate that our H_1 calibration is sufficient to make saturation independent of solvent polarity (Fig. 4) and sample volume and shape (Fig. 6), indicating that the lens effect is not a significant experimental consideration in the analysis of data using line samples.

Effects of Errors in H₁

By varying the microwave power setting P, we have quantitated the H_1-dependence of L''/L and $\int V'_2$ parame-
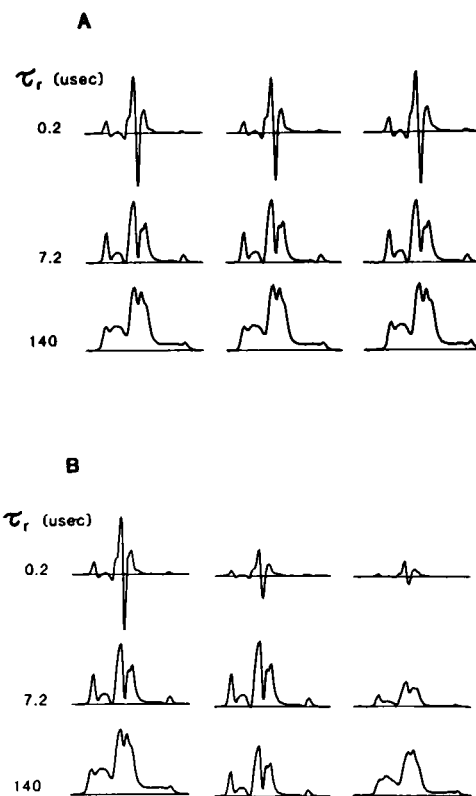

FIGURE 6   Representative ST-EPR (V'_2) spectra obtained for MSL-Hb samples in different types of sample cell, illustrating that correcting for H_1 is sufficient. A: H_1 constant (0.25 G); B: Power (P) constant, where the power for constant H_1 from the small flat cell was used (i.e., top to bottom: 45 mW, 25 mW, and 25 mW). In the vertical direction (top to bottom) τ_r is varied: 0.2, 7.2, and 140 μs. In the horizontal direction, the standard sample cell is varied. These cells are from left to right: small quartz flat cell (3 mm wide × 0.25 mm internal depth), 1 mm i.d. glass capillary, large quartz flat cell (10 mm wide × 0.25 mm internal depth).

ters (Fig. 7). Plots like these were also obtained for the other parameters plotted in Fig. 3. The slope of one of these plots, $\delta X/\delta H_1$, where X is the experimental parameter normalized to its range, is multiplied by $\delta \log \tau_r/\delta X$, from Fig. 3, to obtain an estimate of the H_1-dependent error in measuring τ_r for a given spectral parameter (Table III).

TABLE II
STANDARD ERRORS

Spectral parameter	ST-EPR parameter				
	L''/L	C'/C	H''/H	$\int V'_2$	S'_i
SEM (different sample cells):	0.04	0.05	0.07	0.007	0.05
SEM (same sample cell):	0.02	0.03	0.05	0.008	0.05

Comparison of random errors with errors resulting from the use of different sample cells. ST-EPR parameters are defined in Figs. 2 and 3. The tabulated SEM values are the actual errors in measuring the spectral parameter, averaged over the same hemoglobin samples used in Table I and Fig. 6. Different sample cells here implies a large flat cell with an intercavity volume of ≈ 0.1 ml, and both a small flat cell and a glass capillary with an intercavity volume of ≈ 0.02 ml. All spectra were obtained with $\langle H_1 \rangle = 0.25$ Gauss (Eq. 3).
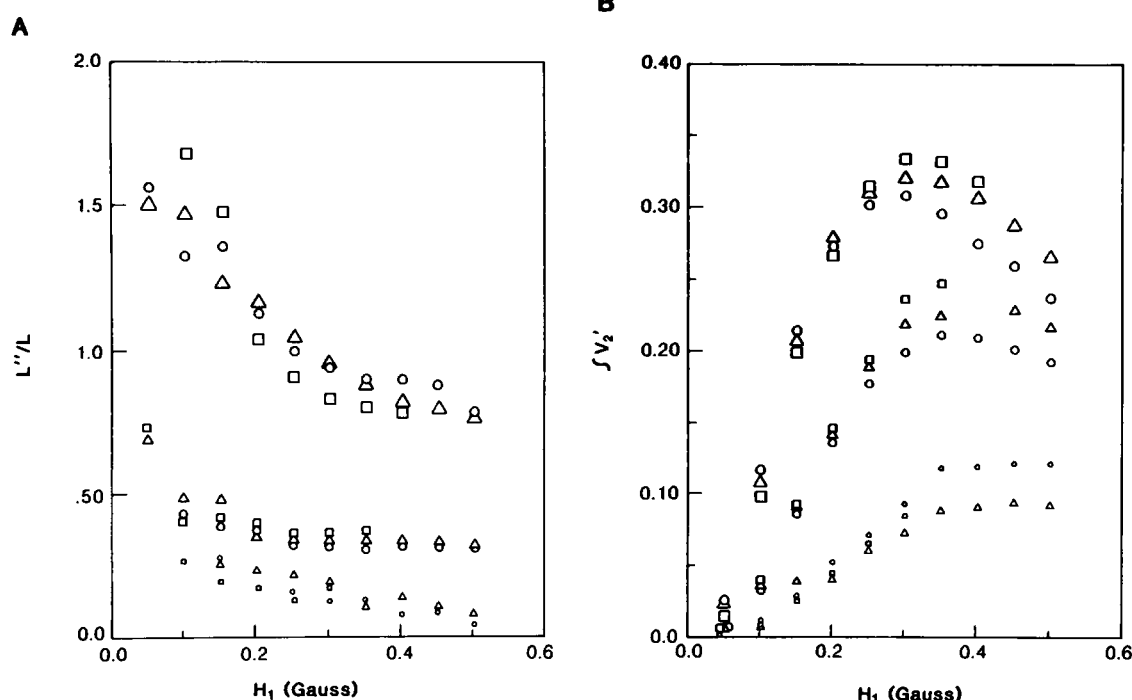
FIGURE 7 Dependence of two ST-EPR (V'_2) parameters on the microwave field strength (H_1). The experimental samples were those described in Fig. 6. L''/L is a lineshape parameter while $\int V'_2$ is an intensity parameter. Other lineshape and intensity parameters had a similar dependence, as shown in Table II.

Note that the V'_2 line-shape parameters L''/L and H''/H are much less sensitive to errors in H_1 than other parameters.

Dependence on O_2

Since saturation should be just as dependent on relaxation times as on H_1 (Eq. 1), it is important to estimate the effects of changing relaxation times on ST-EPR parameters. In Fig. 8, we have used O_2 to alter the relaxation properties of the sample, i.e., to decrease T_1T_2 and thereby decrease saturation (Hyde and Subczynski, 1984). However, O_2 collisions are too infrequent to have significant relaxation effects in the glycerol solutions needed to obtain

TABLE III
EFFECTS OF ERRORS IN H_1 ON ST-EPR PARAMETERS

log τ_r	ST-EPR parameter						
	L''/L	C'/C	H''/H	L''	$\int V'_2$	S'_i	S'_r
−6.68	−0.5	−5	N.D.	0.5	3	5	6
−5.14	−0.6	−4	−0.1	3	8	9	20
−3.85	−2	−4	−2	0.2	4	20	30

The tabulated values are δ (log τ_r)/δH_1, reflecting errors in τ_r due to errors in H_1. Errors in spectral parameters were determined by measuring the slopes of the curves in Fig. 7 (at $H_1 = 0.25\ G$), and the resulting errors in τ_r were then determined from the plots in Fig. 3. The three rows correspond to the same representative hemoglobin samples discussed in Table I and Figs. 6 and 7, having log τ_r values given in column 1. ST-EPR parameters are defined in Figs. 2 and 3. N.D. implies not detectable.
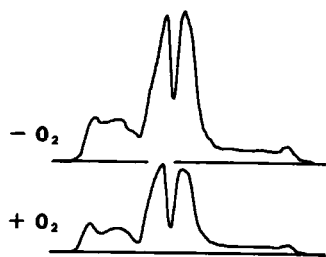
microsecond τ_r values for the hemoglobin model system. Therefore, we analyzed the O_2-dependence of an aqueous sample (the Ca-ATPase from sarcoplasmic reticulum) that has a τ_r in the 10^{-5} s time range (Thomas and Hidalgo, 1978). As shown in Fig. 7 and Table IV, O_2 had little or no effect on the V'_2 line-shape, but the overall intensity (measured by $\int V'_2$) was greatly decreased.

Dependence on Phase

Errors in setting the reference phase on the 100 kHz phase-sensitive detector can affect line-shape parameters, as shown quantitatively in Fig. 9 for a hemoglobin sample (log $\tau_r = -3.85$). In contrast, the V'_2 integrated intensity parameter ($\int V'_2$) has very little phase dependence. Similarly, the other intensity parameters have negligible dependence on phase, as shown in the last four columns of Table V.

Summary of Error Analysis

Table V shows how the three major sources of error quantitated in this study (H_1, W/S, and phase) are expected to contribute to the error in τ_r determination, under optimal experimental conditions. It is assumed that signal/noise is not limiting, that $\tau_r = 10^{-5}$ s (in the center of the motion-sensitive time range), and that procedures are followed to minimize errors in H_1 and phase, as described in Methods. For line-shape parameters, all three sources make similar contributions, while the main source

930

FIGURE 8 Dependence of ST-EPR spectra (V_2') on molecular oxygen. This sample is MSL-Ca-ATPase in sarcoplasmic reticulum at 4°C under nitrogen-purged (*top*) and air-saturating (*bottom*) conditions (see Methods; Table IV).

of error for the last three intensity parameters is H_1. The total propagated errors at the bottom indicate that τ_r can be measured with ~10% precision using line-shape parameters, L'', or $\int V_2'$, but that the in-phase intensity (saturation) parameters S_i' and S_t' have worse precision, due to their sensitivity to H_1 errors. In practice, other errors may become dominant (e.g., W/S may increase), changing the choice of parameter, as discussed further in the Discussion. The propagated errors at the bottom of Table V are quite similar to actual statistical errors obtained from repeated measurements on a single MSL-Hb sample, as shown in Table VI. The precision calculated in Tables V and VI represents the experimental reproducibility under optimal conditions, and therefore represents a lower bound to be used in determining how small a change in τ_r is significant. For example, if the main deviation from these optimal conditions is the presence of a larger W/S component (assumed to be 0.02 in Table V), Table I can be used to estimate the error due to W, and this can be combined with Table V to obtain a new estimate for the precision of τ_r determination.

DISCUSSION

The present study emphasizes the use of spectral intensity parameters in the analysis of ST-EPR spectra, in addition to the more standard line-shape parameters. Our comprehensive model-system study allows us to draw quantitative conclusions about the reliability of the different parame-
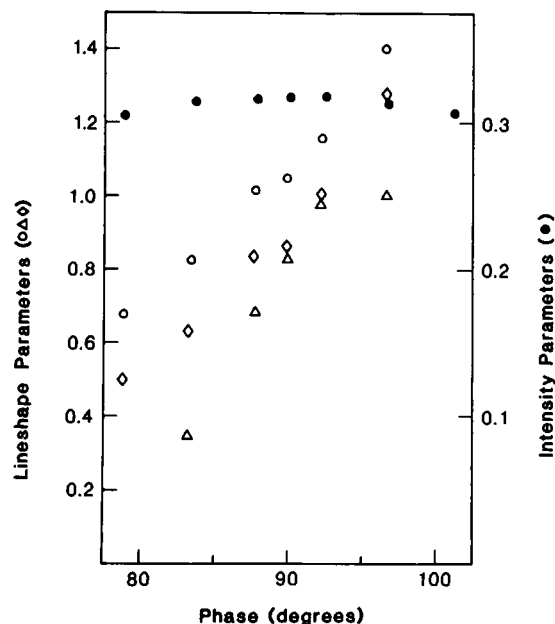

FIGURE 9 Dependence of ST-EPR spectral parameter on errors in setting the reference phase on the phase-sensitive detector. The open symbols are V_2' lineshape parameters: L''/L (O), C'/C (△), and H''/H (◊). The solid circles are $\int V_2'$.

ters, resulting in practical guidelines for the performance and analysis of ST-EPR experiments, including reference spectra and parameter plots (Figs. 2 and 3) that can be used reliably in this analysis. The results (see especially Tables II, IV, and V) demonstrate that line-shape and intensity parameters are complementary to one another, because errors in τ_r-determination are often different for the two types of parameters. Key conclusions are discussed below.

Line-shape parameters offer three principal advantages over intensity parameters. First, they are much less sensitive to molecular oxygen and therefore presumably T_1T_2 (Fig. 8 and Table IV), since O_2 alters the relaxation properties of the spin system through Heisenberg exchange (Subczynski and Hyde, 1984). Second, τ_r values estimated from line-shape parameters have a much smaller dependence on H_1 (Fig. 7 and Tables II and III), the experimen-

TABLE IV
EFFECTS OF O_2

| | ST-EPR parameter[*] | | | |
	L''/L	C'/C	H''/H	$\int V_2'$
(−) O_2	0.86 ± 0.03	0.34 ± 0.06	0.65 ± 0.08	0.26 ± 0.01
τ_r (μs)	(73 ± 8)	(19 ± 5)	(81 ± 23)	(43 ± 10)
(+) O_2	0.84 ± 0.05	0.26 ± 0.06	0.68 ± 0.07	0.18 ± 0.01
τ_r (μs)	(68 ± 13)	(14 ± 3)	(89 ± 22)	(10 ± 3)
τ_r (+O_2)/τ_r (−O_2)[‡]	0.93 ± 0.20	0.74 ± 0.19	1.10 ± 0.41	0.23 ± 0.09

ST-EPR parameters, defined in Figs. 2 and 3, were measured from the spectra of MSL-Ca-ATPase in Fig. 8.
[*]Values represent the mean and standard error of the mean for five measurements.
[‡]Values represent the ratios of the mean values given above.

Error	ST-EPR parameter						
	L''/L	C'/C	H''/H	L''	$\int V'_2$	S'_i	S'_r
$\delta (\log \tau_r)/\delta H_1$	1.1	4.4	0.83	1.3	5.2	10.3	18.5
$\sigma (\log \tau_r)$	0.01	0.05	0.01	0.01	0.05	0.10	0.18
$\sigma (\tau_r)/\tau_r$	0.3	0.11	0.02	0.03	0.13	0.27	0.53
$\delta (\log \tau_r)/\sigma W$	1.5	1.4	0.70	2.1	0.48	0.30	0.12
$\sigma (\log \tau_r)$	0.03	0.03	0.01	0.04	0.01	0.01	0.003
$\sigma (\tau_r)/\tau_r$	0.07	0.07	0.03	0.10	0.02	0.02	0.006
$\delta (\log \tau_r)/\delta \phi$	4.1	5.0	3.9	0.07	0.06	0.00	0.00
$\sigma (\log \tau_r)$	0.02	0.03	0.02	0.0004	0.0004	0.0000	0.0000
$\sigma \tau_r/\tau_r$	0.05	0.07	0.05	0.001	0.001	0.000	0.0000
Total error							
$\sigma (\log \tau_r)$	0.04	0.06	0.03	0.05	0.05	0.10	0.18
$\sigma (\tau_r)/\tau_r$	0.09	0.15	0.06	0.11	0.13	0.27	0.53

Errors in the measurement of τ_r resulting from errors in the major experimental variables H_1, W/S, and phase (ϕ), for the different ST-EPR parameters (defined in Figs. 2 and 3). $\delta (\log \tau_r)/\delta X$ values were measured from the slopes of plots like those in Fig. 7 for H_1 and Fig. 9 for ϕ), in combination with Fig. 2. Optimal experimental conditions were assumed, corresponding to minimal errors in the experimental variables: $\sigma H_1 = 0.01$, $\sigma W = 0.02$, $\sigma \phi = 0.5°$. The individual contributions to the error were then calculated, e.g., for H_1, $\sigma (\log \tau_r) = \sigma H_1 (\delta x/\delta H_1)$, and the propagated error shown at the bottom was calculated from $\sigma^2 = \sigma H_1^2 (\delta x/\delta H_1)^2 + \sigma W^2 (\delta x/\delta W)^2 + \sigma \phi^2 (\delta x/\delta \phi)^2$. Fractional errors in τ_r are also shown.

tal variable most likely to be in error, and this dependence is opposite to the dependence of intensity parameters on H_1 (see below). Third, the spectral resolution of line-shape parameters provides information which can be used to discriminate among different motional models (e.g. heterogeneity or anisotropy; Fajer and Marsh, 1983; Lindahl and Thomas, 1982; Thomas et al., 1985). Thus, under optimal experimental conditions (i.e. no W and a reliable phase setting) line-shape parameters remain the experimental parameters of choice (Tables V and VI).

Intensity parameters offer four principal advantages over line-shape parameters. First, the use of the integrated intensity can improve the accuracy and precision of the measurement, because weakly immobilized probes distort

TABLE VI
PRECISION OF ST-EPR PARAMETERS

	ST-EPR parameter						
	L''/L	C'/C	H''/H	L''	$\int V'_2$	S'_i	S'_r
$\sigma (\log \tau_r)$	0.030	0.048	0.070	0.060	0.070	0.19	0.43
$\sigma (\tau_r)/\tau_r$	0.07	0.12	0.17	0.15	0.18	0.55	2.70

Standard deviations are shown for repeated measurements with the same sample. The same three MSL-Hb samples discussed in Tables I and II were used. The standard deviations were not significantly different for the three samples, so averages of these standard deviations (not SEM values) are given above. These should be compared with the propagated errors predicted in Table V.

lineshapes, but often have minimal integrated intensity (Fig. 4 and 5 and Table I). Second, intensity parameters offer greater signal-to-noise (S/N). Third, they can be added linearly, facilitating the analysis of multi-component systems. Finally, they are insensitive to small phase errors (Fig. 9 and Table V).

Intensity parameters defined at single positions in the spectrum (L'' or S'_r) are spectrally resolved and therefore are sensitive to motional anisotropy, for the same reasons lineshape parameters are sensitive to anisotropy, but have a reduced precision (due to their high sensitivity to H_1; see Tables V and VI) and therefore may mainly prove useful for (a) kinetic studies where the time-dependence of a single spectral position (e.g. L'') is investigated, or (b) cases in which spectral resolution aids in the rejection of W (e.g., S'_r; see below).

The use of intensity parameters to suppress signals due to weakly immobilized probes depends on the mobility and mole fractions of W, the spectrally resolved component corresponding to weakly immobilized probes (Figs. 4 and 5, Table I), and also on the τ_r of the strongly immobilized signal (Table I). Since some ranges of τ_r (W) give rise to large values of integrated intensity parameters ($\int V'_2$ or S'_i) despite small effects on V_1, it is necessary to obtain an estimate of both the τ_r(W) and spin concentration of any weakly immobilized probe in order to determine the applicability of an integrated intensity parameter. Table I should serve as a quantitative guide for this purpose. The integrated V_1 saturation parameter (S'_i) suppresses these signals over a wider range of correlation times than does the integrated V'_2 intensity parameter ($\int V'_2$; see Fig. 5). Therefore, because of its high S/N and superior suppression of W, the integrated in-phase saturation parameter should prove useful when there are weakly immobilized probes present, and/or rapid data acquisition is necessary. However, its relatively poor precision (due to high sensitivity to H_1; Tables V and VI) prevents it from being the parameter of choice. When the mole fraction of W is too high for the effective use of integrated intensity parameters, it would be more appropriate to measure the spectrally resolved S'_i, which is completely resolved from (insensitive to) W. This parameter is a last resort, since its precision is lowest (Table V, VI).

In the present study we have used high-concentration samples, so that the signal to noise ratio (S/N) was not a limiting factor in most cases in determining errors. In practical biophysical studies, however, S/N may be limiting. The increase in S/N for the integrated spectral intensity parameters is largely due to two factors, (a) microsecond motion decreases the intensity at every spectral position, so that some sensitivity is lost by measuring a ratio of intensities at two points, (b) the spectral change is summed throughout the spectrum, not just at one point, thereby magnifying the change in signal intensity, and increasing S/N. Many of the results of this study suggest that H''/H should be the parameter of choice, since it has

low sensitivity to all the major experimental variables (i.e. H_1, W/S, T_1) that result in errors in τ_r (Table V). However H''/H has about seven times lower S/N than L''/L, implying that weak signals would require about 50 times the acquisition time. Even for the high-concentration MSL-Hb samples, the observed error in τ_r from H''/H (Table VI) is three times greater than that predicted from propagated errors that ignore (S/N (Table V), suggesting that S/N is limiting. Thus L''/L remains the parameter of choice when W/S is low, and intensity parameters should be used when W/S is high.

Intensity parameters require constant H_1 and T_1T_2. As discussed above, sensitivity to motion is inherently less for line-shape parameters than for intensity parameters, in which the denominator (normalization factor) is motion-independent. However, the intensity parameters increased sensitivity to motion, and their decreased sensitivity to W and phase, are accompanied by increased sensitivity to other factors affecting saturation, especially H_1 and T_1T_2, which have similar effects throughout the spectrum, and thus affect intensity parameters much more than line-shape parameters (Figs. 7 and 8, Tables III to V). Thus, the advantages of intensity parameters can only be realized if extra care is taken to ensure that H_1 and T_1T_2 are constant. We have described above the procedures necessary to keep H_1 constant. Figs. 2–4 contain reference spectra and parameter plots obtained using these procedures for the line-sample geometry most often used, and therefore should be generally applicable in other laboratories. Since T_1 (Huisjen and Hyde, 1974; Hyde and Dalton, 1979; Fajer et al., 1986 and T_2 (Mason and Freed, 1974) have been found to be roughly constant for correlation times greater than 10^{-8} s in the absence of O_2, it is normally safe to assume that T_1 is unchanging as long as O_2 is absent. However, when possible, time-resolved EPR should be used to verify that the relaxation times are constant. In any case, errors in T_1T_2 and H_1 are unlikely if lineshape and intensity parameters yield similar changes in τ_r values.

Effects of W on line-shape parameters can be similar to those of anisotropic motion. A disagreement between the effective τ_r value determined from different spectral parameters in the V_2' spectrum has frequently been taken as evidence that the motion is anisotropic (Gaffney, 1979; Marsh, 1980; Delmelle et al., 1980. Koole et al., 1981; Johnson et al., 1982; Fajer and Marsh, 1983; Vriend et al., 1984). In fact, the ratio of τ_r values determined from different diagnostic parameters has been proposed as a quantitative measure of the degree of anisotropy (Johnson et al., 1982), and this principle has been supported by theoretical simulations of ST-EPR spectra in the absence of weakly immobilized components (Robinson and Dalton, 1980, 1981; Lindahl and Thomas, 1982; Lindahl et al., 1985). However, the presence of a small population of weakly immobilized probes can affect different diagnostic regions of the spectrum differently (see Fig. 5 and Table I),

and this can easily be mistaken as evidence for anisotropic motion. Horvath and Marsh (1983) have suggested a method to overcome this problem: integrate selected regions of the V_2' spectrum and calculate their ratios. This method, applied either to V_1 or V_2', may offer additional insight into anisotropic motion, but it can only be applicable for weakly immobilized probes [τ_r(W)] in the time window in which the integrated intensity is negligible, as discussed above. Weakly immobilized probes are defined as those that can be resolved in the V_1 spectrum, i.e., τ_r(W) $\leq 10^{-8}$ s and order parameter < 0.4. In these cases, it is often possible to model W and subtract it digitally from the spectrum (Fajer, 1983; Fung and Johnson, 1983; Squier and Thomas, 1985; reviewed in Robinson et al., 1985). However, a heterogeneous population of probes, having different correlation times but rotating isotropically, can also give rise to a spectrum that is consistent with anisotropic motion, even if all probes are strongly immobilized on the V_1 timescale. This is easily seen if the V_2' spectra corresponding to $\tau_r = 10^{-3}$ and 10^{-7} s are added (Fig. 2).

Therefore, in the absence of time-resolved EPR, which would help to resolve different components, unambiguous analysis of anisotropic motion by ST-EPR requires a homogeneous population of probes. It is important to obtain evidence for this through (a) chemical verification of site-selective labeling and (b) variation of conditions during EPR (e.g., variation of temperature or microwave frequency) to detect heterogeneity that might only be spectrally resolved under some conditions.

Summary

The integrated intensity parameters (integral normalized to the number of spins) are particularly useful in the measurement of changes in microsecond probe motions in the presence of some weakly immobilized components (e.g., the temperature dependence of the rotational mobility of the Ca-ATPase; Squier and Thomas, 1986; Bigelow et al., 1986). In addition to the integrated intensity parameters previously used (i.e., $\int V_2'$), in-phase saturation parameters (i.e. S_1' and S_r') are also useful and may be superior under some conditions. The validity of this use of intensity parameters can only be demonstrated if both the mole fraction and mobility of the weakly immobilized probes are quantitatively determined. However, even in the absence of weakly immobilized probes, intensity parameters should complement line-shape parameters, improving the reliability of conclusions drawn from ST-EPR.

REFERENCES

Barlow, A. J., J. Lamb, and A. J. Matheson. 1965. Viscous behavior of supercooled liquids. *Proc. Roy. Soc. A (Lond.)*. 292:322–342.

Benesch, R., G. Macduff, and R. E. Benesch. 1965. Determination of oxygen equilibria with a versatile new tonometer. *Anal Biochem.* 11:81–87.

Bigelow, D. J., T. C. Squier, and D. D. Thomas. 1986. Temperature dependence of the rotational dynamics of protein and lipid in sarcoplasmic reticulum membranes. *Biochemistry.* 25:194–202.

Carrington, A., and A. D. McLachlan. 1979. Introduction to Magnetic Resonance. John Wiley & Sons, New York.

Dalton, L. R. editor. 1985. EPR and advanced EPR studies of biological systems. CRC Press, Boca Raton, Florida.

Delmelle, M., K. W. Butler, and I. C. P. Smith. 1980. Saturation transfer electron paramagnetic resonance spectroscopy as a probe of anisotropic motion in model membrane systems. *Biochemistry.* 19:698–704.

Eads, T. M., D. D. Thomas, and R. H. Austin. 1984. Microsecond rotational motions of eosin-labeled myosin measured by time-resolved anisotropy of absorption and phosphorescence. *J. Mol. Biol.* 179:55–81.

Evans, C. A. 1981. Use of integral of saturation transfer electron paramagnetic spectra to determine molecular rotational correlation times. Slowly tumbling spin labels in the presence of rapidly tumbling spin labels. *J. Magn. Reson.* 44:109–116.

Fajer, P. 1983. Saturation Transfer ESR Spectroscopy Investigation of Lipid Membranes. Ph.d. Dissertation. University of Leeds, Leeds, UK. 242 pp.

Fajer, P., and D. Marsh. 1982. Microwave and modulation field inhomogeneities and the effect of cavity Q in transfer saturation EPR spectra. Dependence on sample size. *J. Magn. Reson.* 49:212–224.

Fajer, P., and D. Marsh. 1983. Sensitivity of saturation transfer EPR spectra to anisotropic rotation. Application to membrane systems. *J. Magn. Reson.* 51:446–459.

Fajer, P., and D. Marsh. 1983. Analysis of dispersion-mode saturation-transfer EPR spectra. Application to model membranes. *J. Magn. Reson.* 55:205–215.

Fajer, P., J. Feix, J. S. Hyde, and D. D. Thomas. 1986. Measurement of rotational molecular motion by saturation recovery EPR. *Biophys. J.* 49(2, Pt. 2):469a (Abstr.)

Fung, L. W. M., and M. E. Johnson. 1983. Multiple motions of the spectrin-actin complex in the saturation transfer EPR time domain. *J. Magn. Reson.* 51:233–244.

Gaffney, B. 1979. Spin label-thiourea adducts. A model for saturation transfer EPR studies of slow anisotropic rotation. *J. Phys. Chem.* 83:3345–3349.

Goldman, S. A., G. V. Bruno, and J. H. Freed. 1973. ESR studies of anisotropic rotational reorientation and slow tumbling in liquid and frozen media. II. Saturation and nonsecular effects. *J. Phys. Chem.* 59:3071–3091.

Hemminga, M. A. 1983. Interpretation of ESR and saturation transfer ESR spectra of spin labeled lipids and membranes. *Chem. Phys. Lipids.* 32:323–383.

Horváth, L. I., and D. Marsh. 1983. Analysis of multicomponent saturation transfer EPR spectra using the integral method: application to membrane systems. *J. Magn. Reson.* 54:363–373.

Huisjen, M., and J. S. Hyde. 1974. A pulsed EPR spectrometer. *Rev. Sci. Instrum.* 45:669–677.

Hyde, J. S., and L. R. Dalton. 1972. Very slowly tumbling spin labels: adiabatic rapid passage. *Chem. Phys. Lett.* 16:568–572.

Hyde, J. S., and L. R. Dalton. 1979. Saturation-transfer spectroscopy. *In*

Spin Labeling. Vol. 2. L. J. Berliner, editor. Academic Press Inc., New York. 1–70.

Hyde, J. S., L. E. G. Eriksson, and A. Ehrenberg. 1970. EPR relaxation of slowly moving flavin radicals: "anamolous saturation." *Biochim. Biophys. Acta.* 222:688–692.

Hyde, J. S., and W. K. Subczynski. 1984. Simulation of ESR Spectra of the Oxygen-Sensitive Spin-Label CTPO. *J. Magn. Reson.* 56:125–130.

Hyde, J. S., and D. D. Thomas. 1973. New EPR methods for the study of very slow motion: application to spin-labeled hemoglobin. *Ann. NY Acad. Sci.* 222:680–692.

Hyde, J. S., and D. D. Thomas. 1980. Saturation-transfer spectroscopy. *Annu. Rev. Phys. Chem.* 31:293–317.

Ibert, M. 1970. Industrial Solvents Handbook. Noyes Data Corp., Park Ridge, New Jersey. 240.

Johnson, M. E., and J. S. Hyde. 1981. 35-GHz (Q-band) saturation transfer electron paramagnetic resonance studies of rotational diffusion. *Biochemistry.* 20:2875–2880.

Johnson, M. E., M. E. L. Lee, and L. W. M. Fung. 1982. Models for slow anistropic rotational diffusion in saturation transfer electron paramagnetic resonance at 9 and 35 GHz. *Biochemistry.* 21:4459–4467.

Keith, A. D., G. Bulfield, and W. Snipes. 1970. Spin-labeled *neurospora* mitochondria. *Biophys. J.* 10:618–629.

Koole, P., and M. A. Hemminga. 1985. Analysis of the Saturation Properties of the Cholestane Spin Label in Oriented Lipid Multilayers in the Gel Phase. *J. Magn. Reson.* 61:1–10.

Kooser, R. G., W. V. Volland, and J. H. Freed. 1969. ESR relaxation studies on orbitally degenerate free radicals. I. Benzene Anion and Tropenyl. *J. Chem. Phys.* 50:5243–5257.

Kusumi, A., W. K. Subczynski, and J. S. Hyde. 1982. Oxygen transport parameters in membranes as deduced by saturation recovery measurements to spin-lattice relaxation times of spin labels. *Proc. Natl. Acad. Sci. USA.* 79:1854–1858.

Lindahl, K., and D. D. Thomas. 1982. Effect of limited rotational motion on simulated conventional and saturation transfer EPR spectra of nitroxide spin labels. *Biophys. J.* 37 (2,Pt.2):71a. (Abstr.)

Lipscomb, J. D., and R. W. Salo. 1983. Electron Paramagnetic Resonance Spectrometer Data Accumulation and Reduction System for Microcomputers. *Comp. Enhanced Spectrosc.* 1:11–15.

Marsh, D. 1980. Molecular motion in phospholipid bilayers in the gel phase: long axis rotation. *Biochemistry.* 19:1632–1637.

McCalley, R. C., E. J. Shimshick, and H. M. McConnell. 1972. The effect of slow rotational motion on paramagnetic spectra. *Chem. Phys. Lett.* 13:115–119.

Ohnishi, S., J. C. A. Boeyens, and H. M. McConnell. 1966. Spin-labeled hemoglobin crystals. *Proc. Natl. Acad. Sci. USA.* 56:809–813.

Polnaszek, C. F., and J. H. Freed. 1975. Electron spin resonance studies of anisotropic ordering, spin relaxation, and slow tumbling in liquid crystalline solvents. *J. Phys. Chem.* 79:2283–2306.

Popp, C. A., and J. S. Hyde. 1981. Effects of oxygen on epr spectra of nitroxide spin-labeled probes of model membranes. *J. Magn. Reson.* 43:249–258.

Robinson, B. H., and L. R. Dalton. 1980. Anisotropic rotational diffusion studied by passage saturation transfer electron paramagnetic resonance. *J. Chem. Phys.* 72:1312–1324.

Robinson, B. H., and L. R. Dalton. 1981. Approximate methods for the fast computation of EPR and ST-EPR spectra V: Application of the perturbation approach to the problem of anistropic motion. *Chem. Phys.* 54:253–259.

Sarna, T., and S. Lukiewicz. 1971. The double role of water in quantitative electron spin resonance (esr) determinations on samples of biological materials. *Folia Histochemica Et Cytochemica.* 9:203–216.

Seidel, J. C. 1973. Effect of actin on the electron spin resonance of spin labeled myosin. *Arch. Biochem. Biophys.* 157:588–596.

Squier, T. C., and D. D. Thomas. 1986. Applications of New ST-EPR methodology to the rotational dynamics of the Ca-ATPase in sarcoplasmic reticulum membranes. *Biophys. J.* 49:937–942.

Stillman, A. E., and R. N. Schwartz. 1976. Heisenberg Exchange in Inhomogeneously Broadened Nitroxide EPR Spectra. *J. Magn. Reson.* 22:269–277.

Subczynski, W. K., and J. S. Hyde. 1984. Diffusion of oxygen in water and Hydrocarbons using an electron spin resonance spin-label technique. *Biophys. J.* 45:743–748.

Thomas, D. D. 1985. Saturation transfer EPR studies of microsecond rotational motions in biological membranes. *In* The Enzymes of Biological Membranes. 2nd edition. vol. I. A. Martonosi, editor. Plenum Publishing Corp. Ch. 8.

Thomas, D. D. 1986. Rotational diffusion of membrane proteins. *In* Techniques for the analysis of membrane proteins. R. J. Cherry and I. Ragan, editors. Chapman and Hall, London.

Thomas, D. D., L. R. Dalton, and J. S. Hyde. 1976. Rotational diffusion studied by passage saturation transfer electron paramagnetic resonance. *J. Chem. Phys.* 65:3006–3024.

Thomas, D. D., T. M. Eads, V. A. Barnett, K. M. Lindahl, D. M. Momont, and T. C. Squier. 1985. Saturation transfer EPR and triplet anisotropy: complimentary techniques for the study of microsecond rotational dynamics. *In* Spectroscopy and the Dynamics of Biological Systems. P. M. Bailey and R. E. Dale, editors. Academic Press, Ltd., London.

Thomas, D. D., J. C. Seidel, J. Gergely, and J. S. Hyde. 1975. The quantitative measurement of rotational motion of the subfragment-1 region of myosin by saturation transfer EPR spectroscopy. *J. Supramol. Struct.* 3:376–390.

Vriend, G., J. G. Schilthuis, J. M. Verduin, and M. A. Hemminga. 1984. Saturation-transfer esr spectroscopy on maleimide spin-labeled cowpea chlorotic mottle virus. *J. Magn. Reson.* 58:421–427.

Weast, R. C., editor. *Handbook of Chemistry and Physics.* 43rd edit. 1961. The Chemical Rubber Co., Cleveland, Ohio. This table does not appear in recent editions. 2227.